Inhibition of HIV-1 Particle Assembly by 2′,3′-Cyclic-Nucleotide 3′-Phosphodiesterase

Sam J. Wilson,[1,2,4,5] John W. Schoggins,[3] Trinity Zang,[1,2,4] Sebla B. Kutluay,[1,2] Nolwenn Jouvenet,[1,2] Mudathir A. Alim,[1,2] Julia Bitzegeio,[1,2] Charles M. Rice,[3] and Paul D. Bieniasz[1,2,4,*]
[1]Aaron Diamond AIDS Research Center
[2]Laboratory of Retrovirology
[3]Laboratory of Virology and Infectious Disease
The Rockefeller University, New York, NY 10016, USA
[4]Howard Hughes Medical Institute, Aaron Diamond AIDS Research Center, New York, NY 10016, USA
[5]Present address: MRC-University of Glasgow Centre for Virus Research, Institute of Infection, Inflammation and Immunity,
University of Glasgow, Glasgow G61 1QH, UK
*Correspondence: pbienias@adarc.org
http://dx.doi.org/10.1016/j.chom.2012.08.012

SUMMARY

The expression of hundreds of interferon-stimulated genes (ISGs) causes the cellular "antiviral state" in which the replication of many viruses, including HIV-1, is attenuated. We conducted a screen for ISGs that inhibit HIV-1 virion production and found that 2′,3′-cyclic-nucleotide 3′-phosphodiesterase (CNP), a membrane-associated protein with unknown function in mammals has this property. CNP binds to the structural protein Gag and blocks HIV-1 particle assembly after Gag and viral RNA have associated with the plasma membrane. Several primate lentiviruses are CNP-sensitive, and CNP sensitivity/resistance is determined by a single, naturally dimorphic, codon (E/K40) in the matrix domain of Gag. Like other antiretroviral proteins, CNP displays interspecies variation in antiviral activity. Mice encode an inactive CNP variant and a single amino acid difference in murine versus human CNP determines Gag binding and antiviral activity. Some cell types express high levels of CNP and we speculate that CNP evolved to restrict lentivirus replication therein.

INTRODUCTION

Type I interferon (IFN) stimulates the expression of hundreds of IFN-stimulated genes (ISGs), causing an "antiviral state" in which the replication of a broad spectrum of viruses, including HIV-1, is inhibited (Ho et al., 1985). A handful of well-characterized ISGs such as APOBEC3G, TRIM5α, and tetherin are known to attenuate retroviral replication in vivo (Kirmaier et al., 2010; Liberatore and Bieniasz, 2011; Okeoma et al., 2007). However, these factors are evaded in their natural hosts or antagonized by viral accessory genes (Neil et al., 2008; Sheehy et al., 2002). Other ISGs, such as ZAP and MOV10, have also been reported to inhibit retroviral replication in vitro (Furtak et al., 2010; Gao et al., 2002).

The contribution of individual ISGs to the overall antiviral state remains largely unclear. We have therefore sought to determine the effect of individual ISGs on HIV-1 replication. Recently, we reported the results of a screen involving nearly 400 human ISGs for their capacity to protect permissive cells from HIV-1 infection (Schoggins et al., 2011). During the screening process we were unable to achieve high levels of transduction with a subset of ISG-encoding HIV-1-based vectors. We hypothesized that some of these ISGs might inhibit infectious lentiviral vector production and, hence, might have specific antiviral activity against HIV-1.

One such ISG is CNP, which encodes 2′,3′-cyclic-nucleotide 3′-phosphodiesterase. CNP-like proteins are present in diverse eukaryotes, and although CNP plays a key role in tRNA splicing in yeast, this is not the case in mammals, where the substrate for CNP and its role in the life of cells is unknown. CNP is expressed at low levels in many mammalian tissues, at higher levels in dendritic cells, and at extremely high levels in oligodendrocytes, which comprise ~40% of the cells in the human brain (Pelvig et al., 2008; Su et al., 2004; Vogel and Thompson, 1988). Here, we demonstrate that CNP can specifically inhibit the generation of infectious particles by several primate lentiviruses, including HIV-1 and HIV-2. We show that CNP binds to Gag and inhibits assembly after Gag has associated with the plasma membrane. The antiviral activity of CNP is highly specific, and naturally occurring single amino acid variations both in the MA region of Gag and in the N-terminal region of CNP are key determinants of CNP antiviral activity. These data suggest that CNP may have evolved to inhibit the propagation of lentiviruses in particular cell types.

RESULTS

CNP Inhibits the Generation of Infectious HIV-1 Particles

We have recently described large-scale screens in which individual ISGs were delivered to cells using bicistronic HIV-1-based vectors (Schoggins et al., 2011). During this study, we identified ~50 ISG-encoding lentiviral vectors that achieved only poor transduction. Although many instances of poor transduction may have been due to cis-acting vector-intrinsic problems, we noted that some genes with previously described antiviral
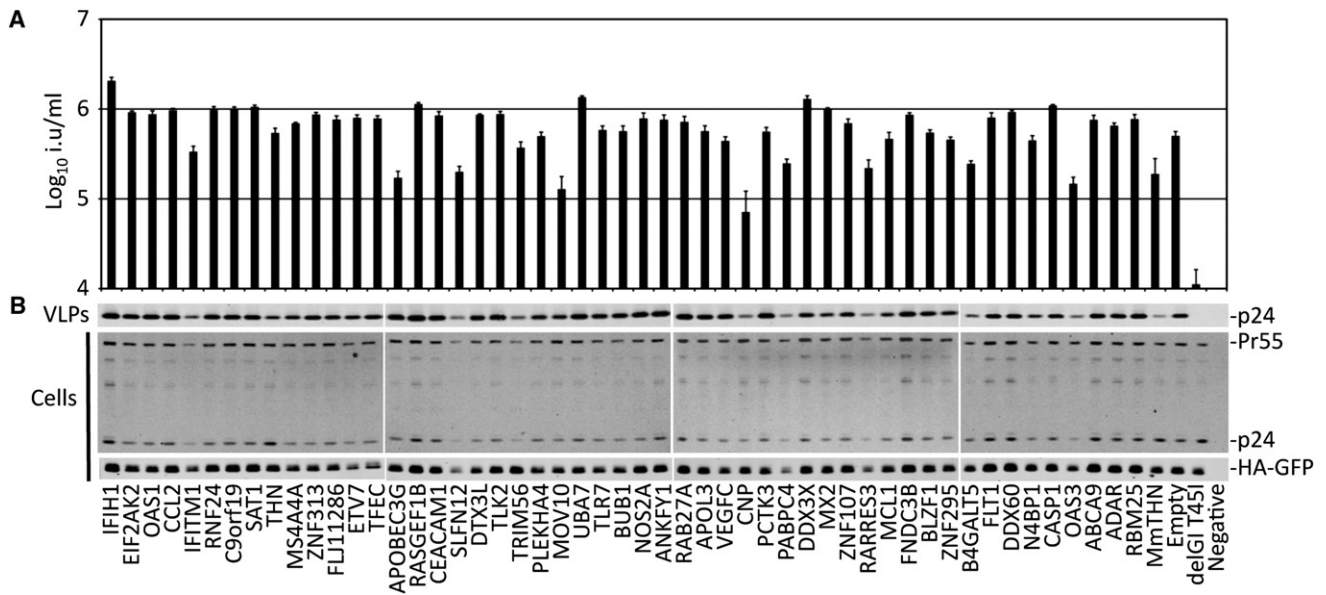
Figure 1. CNP Inhibits HIV-1 in an ISG Screen
(A and B) 293T cells were cotransfected with individual ISG expression vectors (pcDNA DEST40) and the plasmids required to make VSV-G pseudotyped HIV-1 particles. pCMV-HA-GFP was also cotransfected to monitor toxicity. (A) The infectious virion yield was determined by quantifying the number of GFP-positive MT4 target cells using flow cytometry at 48 hr postinfection. Data are represented as mean ± SEM. (B) Pelletable viral CA (p24) abundance in purified supernatants as well as Gag precursor (Pr55), CA (p24), and HA-GFP expression in cell lysates were monitored by western blotting.

activity such as APOBEC3G, tetherin, and MOV10 (Furtak et al., 2010; Neil et al., 2008; Sheehy et al., 2002) were present in this ISG subset. We therefore hypothesized that other genes from this subset might specifically interfere with infectious HIV-1 production.

To investigate this possibility, we subcloned these ~50 ISGs into a conventional mammalian expression plasmid and measured their ability to inhibit infectious HIV-1-based lentiviral vector production when expressed in *trans* (Figure 1A). Simultaneously, HIV-1 Gag protein expression in cells and particulate capsid (CA) protein in culture supernatant was monitored by western blotting (Figure 1B). Control antiviral genes, specifically Rhesus macaque tetherin (MmTHN; Figures 1A and 1B) and human tetherin mutated to resist Vpu-antagonism (delGI T45I) (McNatt et al., 2009), reduced infectious particle yield without affecting Gag expression (Figures 1A and 1B).

Conversely, most of the ~50 screened ISGs had little effect on HIV-1 vector production (Figure 1A). Human tetherin, a well-characterized antiviral restriction factor (Neil et al., 2008) had only a modest effect because the GagPol expression vector used also encodes Vpu, which antagonizes its activity. Of the genes that did reduce infectious virion yield, most decreased the levels of both Gag and coexpressed HA-green fluorescent proteins (GFP) (e.g., SLFN12, RARRES3, or OAS3) (Figure 1B). This was likely a result of global or nonspecific effects, induced by expressing these genes.

The screen correctly identified APOBEC3G and MOV10 as antiviral ISGs, both of which reduced infectious virion yield without inhibiting Gag expression or physical particle production, (Furtak et al., 2010; Sheehy et al., 2002). Notably, we also found that one additional ISG, CNP, also substantially inhibited infectious particle production (Figure 1A). This effect of CNP

occurred in the absence of any defect in Gag protein expression (Figure 1B). However, in contrast to APOBEC3G and MOV10, and like tetherin, CNP reduced the abundance of particulate CA protein in the supernatant of transfected cells, suggesting that CNP functioned at a stage of the virus replication cycle between Gag expression and virion release.

CNP Inhibits Replication-Competent HIV-1 at Physiological Expression Levels

To determine whether CNP could inhibit replication competent HIV-1 in the presence of the normal repertoire of accessory proteins, we coexpressed an HIV-1 proviral plasmid (NL4-3) with varying amounts of CNP. Infectious particle production was decreased in a CNP dose-dependent manner, with ~100-fold reduction in infectious virion yield at the highest level of CNP expression (Figure 2A). In accordance with findings during the initial screen (Figure 1), CNP expression substantially reduced particulate CA protein in the supernatant of transfected cultures by, up to ~10- to 50-fold (Figures 2B, S1A, and S1B available online), but did not affect the total level of cell-associated Gag protein (Figure 2C). However, Gag processing appeared to be reduced in cells coexpressing CNP, as the presence of CNP led to an apparent ~2-fold reduction in cell-associated CA protein and a corresponding increase in the levels of unprocessed Pr55 Gag precursor in cell lysates (Figure 2C). This apparent reduction in cell-associated Gag processing was likely a secondary effect of decreased particle assembly, because CA protein in released virions was processed normally (Figure 2B). Furthermore, no defect in intrinsic particle infectiousness, or envelope incorporation into virions, was observed in the presence of CNP (Figure S1C), again suggesting that CNP affected the quantity and not the quality of the particles that were released.
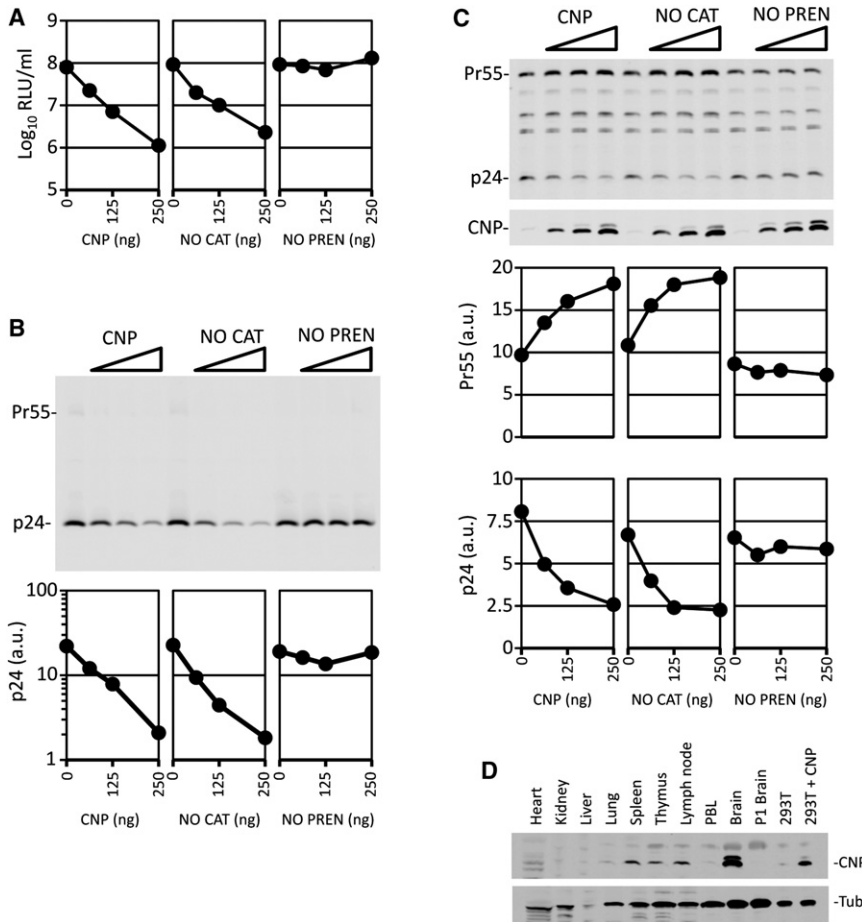
Figure 2. Expression of Catalytically Active or Inactive, but Not Prenylation-Defective, CNP at Physiological Levels Reduces Infectious HIV-1 Viron Yield and Gag Processing

(A) 293T cells were cotransfected with an HIV-1 proviral plasmid (pNL4-3) and increasing amounts of plasmids expressing CNP, catalytically inactive CNP (NO CAT), and CNP lacking a prenylation CAAX box (NO PREN). At 48 hr posttransfection, infectious virion yield was measured using TZM-bl indicator cells and is plotted as relative light units (RLU) per ml.

(B and C) Quantitative western blot analysis (LiCOR) of virion-associated CA (p24) abundance (B), and cell-associated Gag expression/processing (C) was monitored. Charts below the blots show quantitation of the Pr55 and/or p24 signal in each lane of the virion (B) and cell lysate (C) western blots.

(D) Expression of CNP in mouse tissues and transfected 293T cells was analyzed by western blotting. Blots were also probed with anti-tubulin (Tub) as a loading control. See also Figure S1.

lymph node (Figure 2D), raising the possibility that cells expressing inhibitory levels of CNP might also reside in these tissues.

Several, but Not All, Mammals Encode a CNP that Can Inhibit a Subset of Lentiviruses

Because retroviral restriction factors often display species-dependent variation in antiviral activity that can be exploited in their characterization, we tested CNP from a panel of mammalian species for their ability to inhibit a panel of retroviruses. Comparable levels of all CNP variants were expressed (Figures 3A–3H) and most of those tested (macaque, African green monkey, cow, and sheep) exhibited antiretroviral activity. However, murine CNP was inactive against any of the viruses tested (Figures 3A–3H).

With the exception of murine CNP, the spectrum of viruses targeted by CNP was the same for all the variants tested (Figures 3A–3H). Primate lentiviruses such as $SIV_{MAC}239$ (Figure 3B), HIV-2 7312A (Figure 3D) and $SIV_{AGM}SAB$ (Figure 3E) were all sensitive to CNP to varying degrees. Indeed, $SIV_{MAC}239$ seemed particularly sensitive to inhibition by CNP, with infectious particle production being reduced over 100-fold when coexpressed with multiple CNP variants (Figure 3B). Furthermore, the apparent inhibition of HIV-1 Gag processing, evident in the presence of CNP (Figures 2C and Figures 3A), was more striking in the case of $SIV_{MAC}239$ (Figure 3B). Indeed, processed $SIV_{MAC}239$ CA was barely detectable in the presence of inhibitory variants of CNP.

The specificity of CNP-mediated inhibition was highlighted by the resistance of both the nonprimate lentivirus FIV (Figure 3G) and the gammaretrovirus MLV (Figure 3H). Furthermore, CNP was able to distinguish between closely related viruses. For example, $SIV_{MAC}239$ and HIV-2 7312A were sensitive to multiple CNP variants (Figures 3B and 3D) whereas HIV-2 ROD10 was

CNP possesses well-defined catalytic activity (Lee et al., 2001) and also contains a CAAX box prenylation signal at its C terminus, which is thought to drive membrane localization. Catalytically inactive mutant CNP (H251A, T253A, H330A, T332A) inhibited virion production as effectively as wild-type (WT) CNP (Figures 2A–2C). In contrast, introduction of a point mutation (C418A) into the prenylation motif had little effect on CNP expression levels, but abolished antiviral activity (Figures 2A–2C). These data suggest that CNP prenylation is essential, but catalytic activity is dispensable, for inhibition of HIV-1 production.

CNP is only weakly induced by type I IFNs (Bartee et al., 2009); we therefore assessed CNP expression levels in various tissues to determine whether any expressed sufficient levels to inhibit particle production in vivo (Figure 2D). Note that the two forms of CNP visible in Figures 2C and 2D and throughout this study are generated from alternate translation initiation codons (O'Neill et al., 1997) (see also Figure 4A). In accordance with the use of CNP as a marker of differentiated oligodendrocytes (Vogel and Thompson, 1988), CNP was abundantly expressed in brain tissue from adult mice (Figure 2D). Notably, expression levels in adult brain tissue exceeded the maximum level of coexpressed CNP used in transfected 293T cells (Figure 2). Thus, CNP expression levels in oligodendrocytes greatly exceeded those required to observe antiviral activity. Interestingly, significant CNP expression was detected in spleen, thymus, and
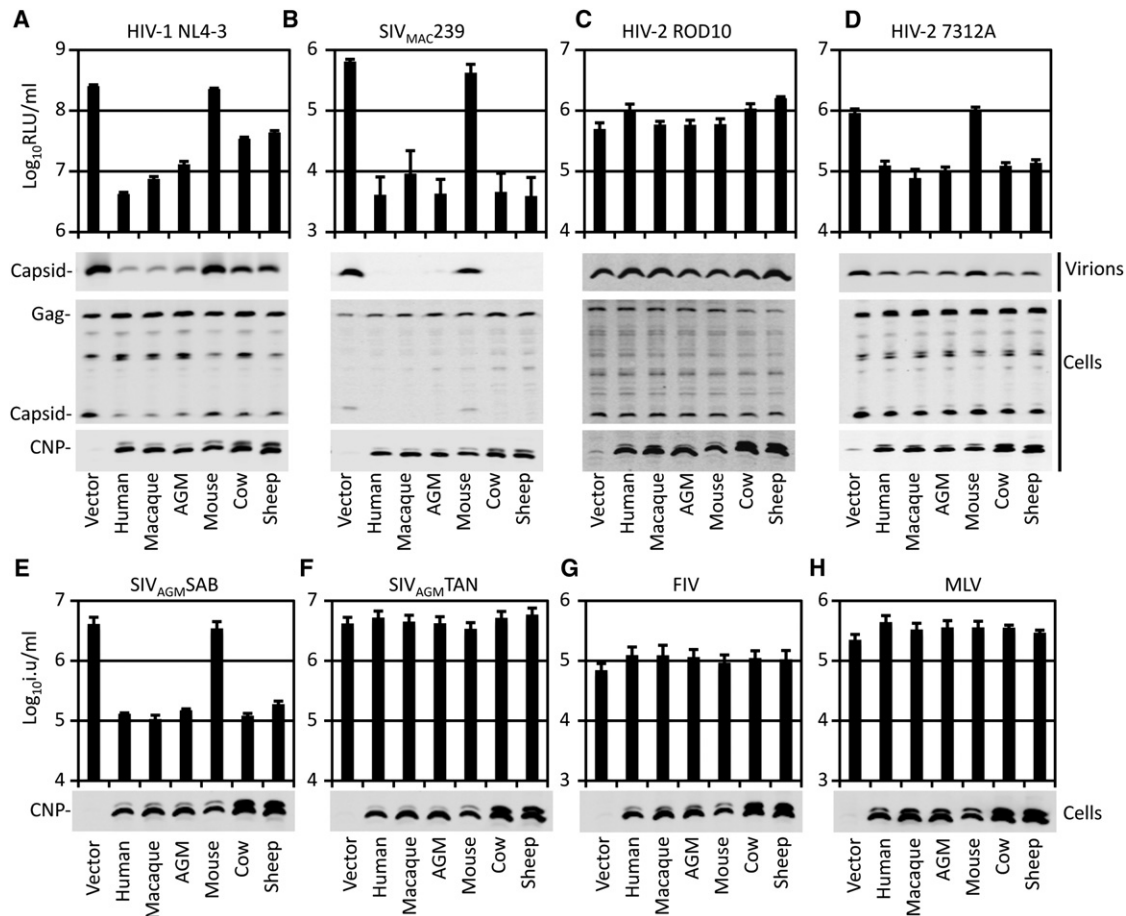
Figure 3. Spectrum of Antiviral Activity Exhibited by CNP

(A–H) 293T cells were transfected with expression vectors encoding CNP from: *Homo sapiens* (Human), *Macaca mulatta* (Macaque), *Chlorocebus aethiops* (AGM), *Mus musculus* (mouse), *Bos torus* (cow), *Ovis aries* (sheep), or an empty vector control, in combination with proviral clones (A–D) or plasmids required to generate single-cycle vectors (E–H). Data are represented as mean ± SEM. At 48 hr after transfection, supernatants were harvested and yields of infectious HIV-1 (A), SIVmac239 (B), HIV-2 ROD10 (C), or HIV-2 7312A were monitored using TZM-bl target cells, as in Figure 2A. Yields of infectious VSV-G pseudotyped GFP-encoding vectors were determined by titration on MT4 cells for SIV$_{AGM}$SAB (E), SIV$_{AGM}$TAN (F), FIV (G), or MLV (H). Gag (A–D) and CNP (A–H) expression in cell lysates, and particulate CA protein in supernatants (A–D) was monitored by western blotting.

completely resistant (Figure 3C). Similarly, whereas SIV$_{AGM}$SAB was inhibited by CNP, SIV$_{AGM}$TAN was unaffected (Figure 3F). Importantly, these data indicate that the antiviral activity of CNP is specific to particular retroviruses, and is therefore unlikely to be due to generalized perturbation of cell physiology.

A Single Amino Acid Residue that Differs in Murine CNP Is Required for Antiviral Activity

The observation that murine CNP lacked antiviral activity against the viruses tested led us to investigate which CNP domains were critical for its activity. We used SIV$_{MAC}$239 in these experiments because it was particularly sensitive to CNP (Figure 3B). Human CNP is a 422 amino acid protein that shares ∼85% amino acid identity with murine CNP (Figure 4A). We first constructed chimeric CNP molecules by exchanging amino acids 1–224 of mouse and human CNP (Figure 4B). A chimeric CNP encoding murine N-terminal and human C-terminal domains (MmHs) had no antiviral activity, whereas the reciprocal chimera (HsMm)

was fully active (Figure 4C). Thus, determinants of the antiretroviral activity of CNP mapped to the N-terminal half of CNP, which includes the P loop domain.

Most of the differences between human and murine CNP N termini were confined to three regions encompassing amino acids 69–75, 89–99, and 109–118 (Figure 4A). Replacing amino acids 69–75 (but not amino acids 89–99 or 109–118) in human CNP with murine counterparts abolished antiretroviral activity, without affecting expression level (Figures 4 and 4C). Moreover, when individual amino acid substitutions were made in this region, a single conservative substitution (D72E, effectively a three atom [CH$_2$] insertion into the amino acid side chain) rendered human CNP completely inactive, without affecting expression levels (Figures 4B and 4C). Although the identity of residue 72 was critical for CNP activity, it was not the sole determinant because the corresponding E72D change in murine CNP failed to confer CNP antiviral activity (data not shown).
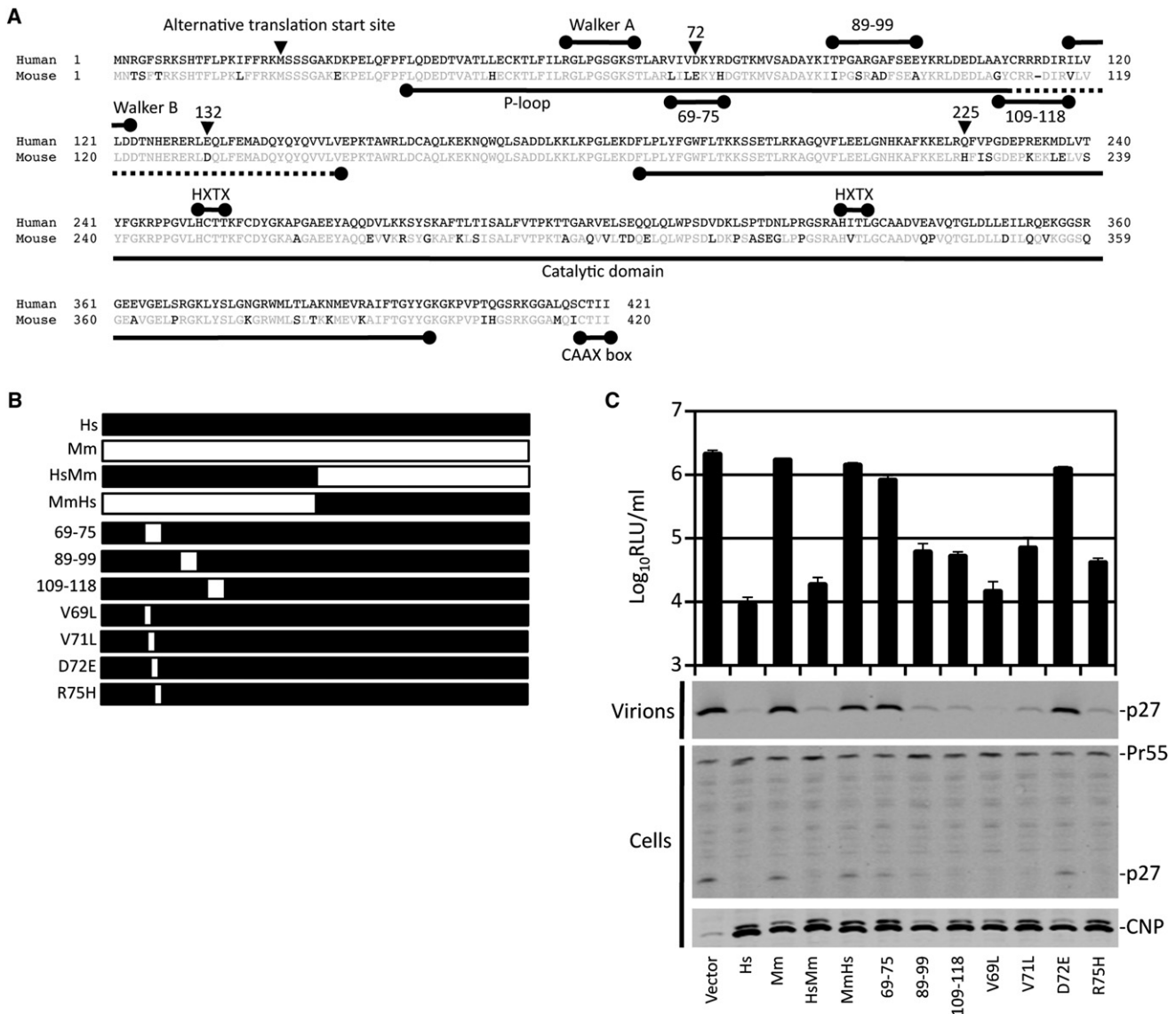
Figure 4. A Single Amino Acid in the N-Terminal P Loop Domain Confers the Antiviral Activity of CNP

(A) Alignment of human and murine CNP proteins, with salient features annotated.

(B and C) 293T cells were cotransfected with a SIV$_{MAC}$239 proviral plasmid along with plasmids expressing human CNP, mouse CNP, or mutants thereof (B). The CNP proteins tested included human-mouse chimeras (HsMm and MmHs); human CNP containing regions of murine sequence (69–75, 89–99, and 109–118); and human CNP containing single point mutations (V69L, V71L, D72E, and R75H). (C) At 48 hr posttransfection, infectious virion yield was quantified by titration on TZM-bl cells. Data are represented as mean ± SEM. Virion-associated CA (p27) as well as CNP and Gag expression/processing in cell lysates was monitored by western blotting.

CNP Targets the MA Domain of the HIV-1 Gag Protein Following Its Association with the Plasma Membrane

The fact that Gag expression is sufficient to drive VLP formation led us to consider whether CNP might directly target Gag. In fact, CNP inhibited the production of VLPs assembled using either native codon or codon-optimized (synGag) Gag expression plasmids, without affecting Gag protein expression levels (Figure 5A). Because synGag expression is achieved in the absence of HIV-1 genomic RNA sequences, this result suggested that CNP acts against HIV-1 Gag directly, with no requirement for any other virally encoded component.

The moderate Gag processing defect that was observed under conditions where CNP reduced particle yield (Figures 2C, Figures 3A, and 3B) is reminiscent of the effects of MA mutations that reduce membrane binding (Bryant and Ratner, 1990) suggesting the possibility that CNP might target MA. Indeed, particle formation driven by an HIV-1 Gag construct, Gag-δGH, which lacks the majority of MA (amino acids 7–110) (Perez-Caballero et al., 2004), was resistant to inhibition by CNP (Figure 5B). Based on these results, we next examined whether transferring the MA region of HIV-1 to MLV, a virus that is ordinarily CNP-resistant, (Figure 3H), might confer sensitivity. Indeed,
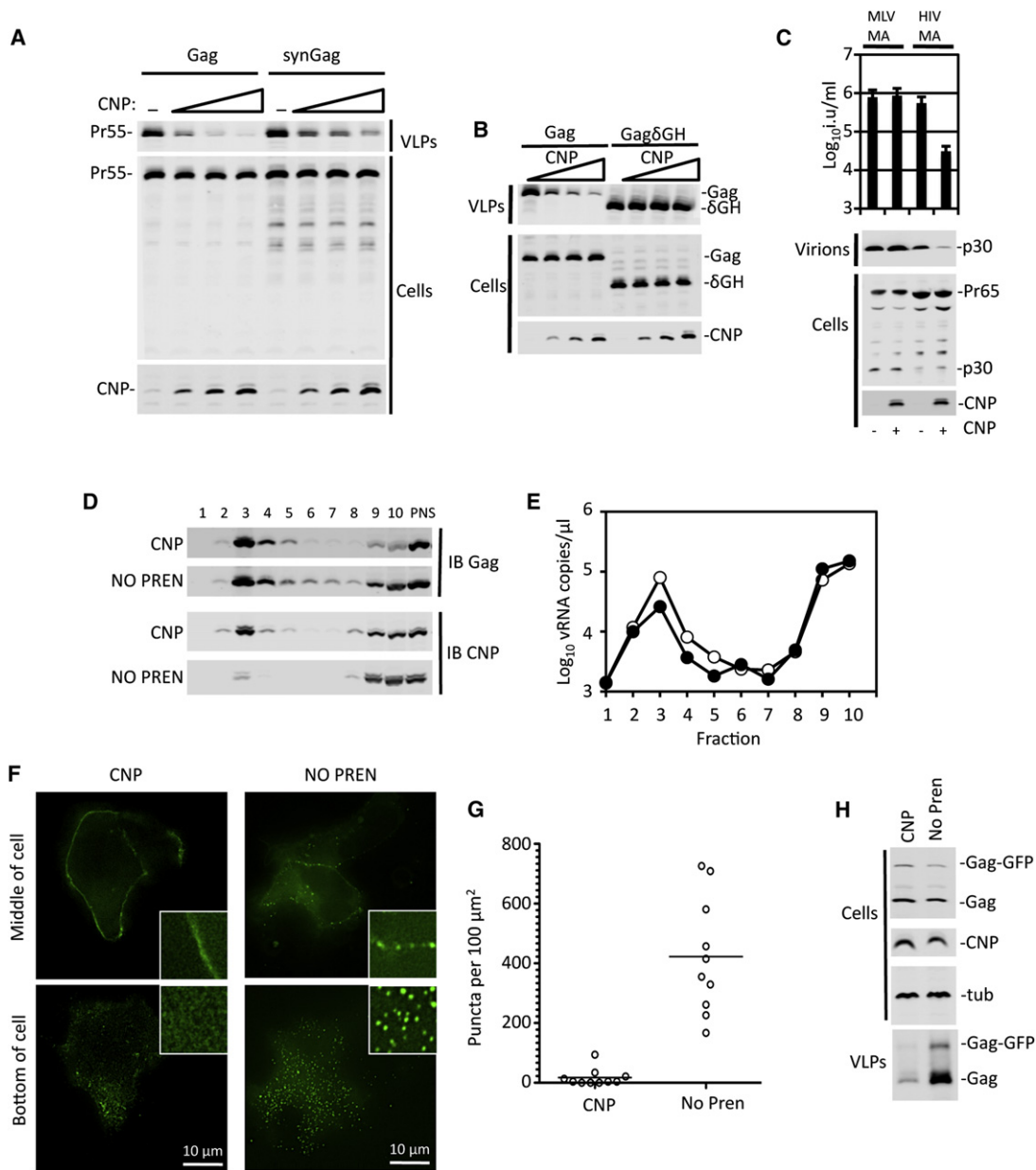
Figure 5. CNP Targets the MA Domain of HIV-1 Gag and Block Assembly after Gag Reaches the Plasma Membrane

(A) Effect of CNP on VLP production driven by native codon (Gag) or codon optimized (synGag) expression, as determined by western blot analyses of 293T cell cultures transfected with Gag and CNP expression plasmids.

(B) Effect of CNP on VLP production driven by HIV-1 Gag or Gag δGH expression, as determined by western blot analyses of 293T cell cultures transfected with Gag and CNP expression plasmids.

(C) Effect of CNP on VLP production driven by plasmids required to make VSV-G pseudotyped single cycle MLV vectors, using either an MLV GagPol expression plasmid or MLV GagPol in which MA was substituted with HIV-1 MA. Infectious virion yield was quantified by titration on MT4 cells Data are represented as mean ± SEM. Particulate MLV CA in culture supernatants as well as CNP and Gag expression/processing in cell lysates were assessed by western blotting.

(D) Western blot analysis of CNP and HIV-1 Gag abundance after fractionation (lanes 1–10) of 293T cell lysates on a membrane flotation gradient following cotransfection with plasmids expressing HIV-1 Gag, a packageable HIV-1 vector genomic RNA and CNP or nonprenylated CNP (NO PREN). PNS, unfractionated postnuclear supernatant.

(E) Viral genomic RNA abundance determined by RT-qPCR analysis of the same fractions as in (D) is shown.

(F) Representative images of 293T cells 24 hr after cotransfection with plasmids expressing either CNP or CNP lacking a prenylation sequence (NO PREN), along with plasmids encoding Gag and Gag-GFP (in a 5:1 ratio).

(G) Quantification of fluorescent puncta in three fields from ten randomly selected Gag/Gag-GFP and CNP expressing cells. The number of puncta per 100 μm^2 for each individual cell is plotted. Horizontal lines represent mean values.

(H) Western blot analysis of Gag, CNP, and α-tubulin expression in cells, and VLP abundance in culture supernatants for cells treated identically to those examined in (F) and (G).

this manipulation conferred CNP-sensitivity, and CNP reduced the yield of infectious virions assembled using the chimeric Gag by ∼50-fold (Figure 5C). Thus, the MA region of Gag is the key determinant of sensitivity to CNP.

The efficiency of Gag multimerization, and thus assembly, is greatly enhanced by Gag association with both the plasma membrane (Kutluay and Bieniasz, 2010) and with viral or cellular RNAs. Because (1) MA directs Gag to membranes and was a key determinant of CNP sensitivity (Figures 5B and 5C), (2) CNP is a membrane-anchored RNA binding protein, and (3) the CNP membrane anchor (prenylation) was essential for antiviral activity (Figure 2), we investigated whether CNP affected the ability of HIV-1 Gag to associate with membranes, or inhibited the ability of Gag to recruit HIV-1 genomic RNA. Interestingly, under conditions where particle assembly was blocked by CNP, there was little effect on the subcellular distribution of Gag, as assessed by fractionation of Gag-expressing cells on a membrane flotation gradient (Figure 5D). Specifically, Gag was readily detectable in the membrane fraction (fraction 3) of cells coexpressing either WT CNP or inactive nonprenylated CNP (Figure 5D). In contrast, the abundance of the nonprenylated mutant of CNP in membrane fractions was greatly diminished (Figure 5D). These data indicate that even though MA is a key sensitivity determinant, CNP does not inhibit the ability of Gag to associate with membranes. Nonetheless, CNP-membrane association seemed to be required for antiviral activity.

We previously described an assay in which RT-qPCR is coupled with membrane flotation analysis to measure the distribution of HIV-1 RNA in infected cells (Kutluay and Bieniasz, 2010). Using this assay, we found that CNP did not affect the ability of Gag to recruit genomic RNA to membranes (Figure 5E). Overall, these findings indicated that CNP inhibits particle production subsequent to a key early event in virion assembly, namely the association of Gag and viral genomic RNA with the plasma membrane.

To further delineate the step at which CNP acts, we used a microscopy-based approach. Assembly of morphologically accurate, individual HIV-1 VLPs can be readily visualized by fluorescence microscopy using coexpressed Gag and Gag-GFP fusion proteins (Jouvenet et al., 2008; Larson et al., 2005). Normally, Gag-GFP that is initially diffuse concentrates at sites of virion assembly, forming bright fluorescent puncta. In the presence of nonprenylated, inactive CNP, distinctive puncta of Gag-GFP could be readily observed (Figure 5F) and quantified (Figure 5G). Moreover, extracellular VLP production proceeded efficiently (Figure 5H). However, in the presence of CNP, a striking paucity of puncta was observed on the cell surface (Figure 5F). Quantitative analysis revealed that the abundance of VLPs had been reduced ∼20-fold by CNP coexpression (Figure 5G). A simultaneous, dramatic reduction in extracellular VLP yield was also observed, whereas the overall level of Gag/Gag-GFP expression was unaffected by CNP (Figure 5H). Once again, Gag-GFP accumulation at the plasma membrane appeared abundant even in the presence of CNP, however, the Gag-GFP was diffusely distributed at the plasma membrane and failed to coalesce into puncta (Figure 5F). These data reinforce the conclusion that CNP inhibits HIV-1 virion assembly subsequent to the association of Gag with the plasma membrane.

Selection of a CNP-Resistant HIV-1 Mutant

The rapidity of HIV-1 evolution often makes it possible to isolate mutants in vitro that are resistant to inhibitors. We asked whether HIV-1 could evolve resistance to CNP following cultivation in the presence of CNP. Derivatives of MT4 T cells expressing similar levels of either active CNP or inactive (nonprenylated) CNP were generated (Figure 6A) and then infected with a replication-competent HIV-1 clone in which Nef was replaced with EGFP (NHG, GenBank accession number: JQ585717). MT4 cells are unusually permissive to HIV-1 replication, and unmodified cells, or cells expressing nonprenylated CNP, became nearly 100% infected between day 3 and day 4 after inoculation (Figure 6B). However, HIV-1 replication was delayed in MT4 cells expressing the intact CNP protein, with the majority of cells remaining uninfected on day 5 (Figure 6B). This result highlights the ability of CNP to inhibit the spread of HIV-1.

HIV-1 propagated in the presence of CNP was harvested on day 6, and following three subsequent passages in MT4 cells expressing CNP, an isolate was obtained that replicated with indistinguishable kinetics in the presence or absence of CNP (Figure 6C). Interestingly, this CNP-adapted isolate also replicated with near-identical kinetics to the parental HIV-1 clone in unmodified MT4 cells (Figures 6B and 6C). Sequencing of PCR-amplified proviral *gag* DNA identified a single G to A transition that had apparently been selected to near uniformity in the CNP-resistant isolate. This single nonsynonymous change altered codon 40 in the MA region of Gag from glutamate (5′-GAG-3′) to lysine (5′-AAG-3′) (Figure 6D). This change is henceforth referred to as E40K. When this single amino acid change was introduced into the parental HIV-1 clone, replication in primary lymphocytes was impaired only marginally in one donor, and not at all in a second (Figure 6E). Moreover, the E40K mutation did not substantially alter envelope incorporation into virions (Figures S2A–S2C). This suggested that resistance to CNP was acquired without incurring a major replicative fitness cost.

Importantly, the E40K mutation was sufficient to confer complete resistance to the inhibitory effects of CNP on infectious virion production from both 293T cells (Figure 6F) and MT4 cells (Figures S2D and S2E). E40 is exposed on the surface of the globular head of myristoylated MA (Tang et al., 2004), and is positioned close to, but not precisely coincident with the positively charged surface that is thought to participate in membrane binding (Figure 6G). Moreover, E40 is positioned toward the interior of the trimer structure that is adopted by MA in crystals (Hill et al., 1996). A survey of the variation at E40 in an alignment of primate lentiviruses (http://www.hiv.lanl.gov) revealed that this position is dimorphic in primate lentiviruses and the amino acid identity at this position (Figure 6D) correlated precisely with primate lentivirus sensitivity to CNP (Figure 3). Whenever E40 was present, the virus was sensitive to CNP (HIV-1, SIV$_{MAC}$239, SIV$_{AGM}$SAB, and HIV-2 7312A), and whenever K40 was present, the virus was resistant (HIV-2 ROD10 and SIV$_{AGM}$TAN) (Figures 3 and Figures 6D). Taken together, these data strongly suggest that HIV-2 ROD10 and SIV$_{AGM}$TAN are resistant to CNP because they encode a lysine residue at the equivalent position to HIV-1 E40K. Notably, the vast majority of primate lentiviruses encode glutamate at position 40 and are therefore predicted to be CNP sensitive. Only rare examples of HIV-2, SIV$_{AGM}$, and SIV$_{RCM}$ encode K40 and are therefore predicted to be CNP-resistant.
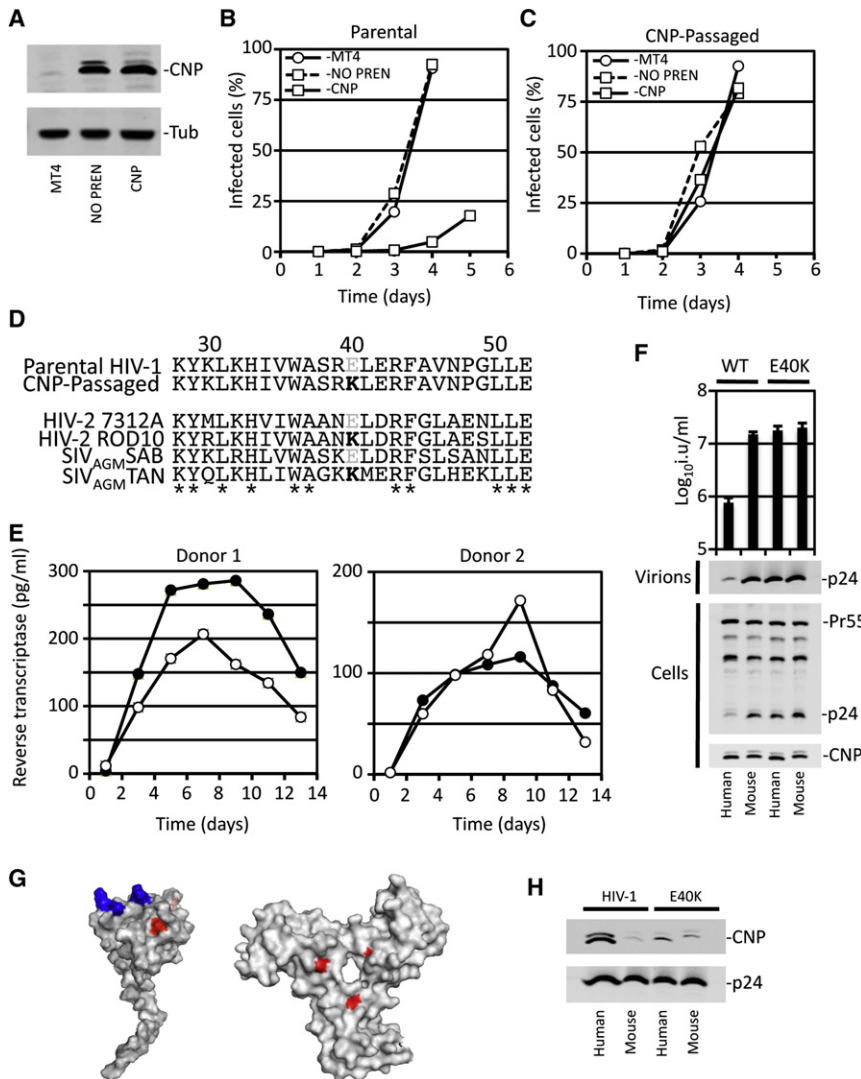
Figure 6. Selection and Characterization of a CNP-Resistant HIV-1 Gag Mutant

(A) Western blot analysis of CNP expression in MT4 cells stably expressing intact CNP, or CNP lacking a prenylation sequence (NO PREN), generated by retroviral transduction.

(B and C) Replication of GFP-encoding HIV-1 (NHG) (B), or NHG passaged on CNP expressing cells (C), on CNP-expressing MT4 cells is shown, as the percentage of infected cells determined by flow cytometry.

(D) An alignment primate lentiviral MA sequences encompassing the E40K (highlighted) substitution, numbered according to HIV-1 (NL4-3).

(E) Replication of WT (filled symbols) and E40K mutant (open symbols) HIV-1 (NHG) in peripheral blood mononuclear cells from two donors, monitored by assaying reverse transcriptase activity in culture supernatants.

(F) Infectious virion yield, quantified by titration on MT4 cells following cotransfection of 293T cells with plasmids expressing CNP along with WT or E40K mutant NHG. Data are represented as mean ± SEM. Virion-associated CA (p24) as well as CNP and Gag expression/processing in cell lysates was monitored by western blotting.

(G) A structural representation (Protein Data Bank [PDB] ID: 1UPH) of the monomer myristoylated MA region of Gag (Tang et al., 2004). Basic residues from the MA basic region are highlighted in blue and the dimorphic position 40 is highlighted in red. Also shown is the trimeric crystalline form of MA (PDB ID: 1HIW) with position 40 highlighted in red (Hill et al., 1996).

(H) Purified HIV-1 virions from the experiment shown in (F) were normalized for p24 content, and subjected to western blot analysis using antibodies to p24 and CNP. See also Figure S2 and Table S1.

CNP is expressed at low, subinhibitory levels in many cell types. For example, CNP is barely detectable in 293T cells (Figure 2). Nevertheless, CNP is among the more abundant proteins detected by mass spectroscopic analysis of purified HIV-1 virions derived from 293T cells (Table S1) and is also found in macrophage-derived virions (Chertova et al., 2006). Therefore, we examined the degree to which CNP was incorporated into HIV-1 particles when expressed at inhibitory levels, using the active (human) and inactive (murine) CNP proteins as well as sensitive (E40) and resistant (K40) HIV-1 strains. Because overexpressed CNP inhibits the assembly of WT HIV-1, there were fewer particles generated by cells coexpressing human CNP (Figure 6F). However, when equal numbers of virions were analyzed (based on particulate CA quantities, Figure 6H), human CNP was easily detected in WT virions, whereas the inactive murine CNP was largely absent (Figure 6H). In addition, CNP was also largely absent from E40K mutant virions. Importantly, virion-associated CNP was resistant to digestion by subtilisin indicating that it is packaged into the interior of virions (Figure S2F). Together, these data suggest that CNP associates with virions, specifically when active CNP and a CNP-sensitive Gag protein are present and is efficiently incorporated into virions if assembly is completed.

CNP Binds Directly to HIV-1 Gag and Blocks an Early Step in Virion Assembly

To further examine whether CNP associates with assembling virions, we used fluorescent microscopy to determine whether CNP and Gag-mCherry fusion proteins colocalize in transfected cells. Because antiviral doses of CNP inhibit the formation of Gag puncta (Figures 5F and 5G) that would complicate analyses of colocalization, we used a low, subinhibitory dose of coexpressed CNP. A high degree of colocalization between CNP and Gag-mCherry was observed, with a mean Pearson's colocalization coefficient of ~0.6 (Figures 7A and 7C). Notably, CNP exhibited a greatly reduced degree of colocalization with the CNP-resistant E40K Gag mutant, with a mean colocalization coefficient value of ~0.2 (Figures 7B and 7C). The data suggest that WT, but not CNP-resistant, Gag recruits CNP to sites of particle assembly.

Cumulatively, our findings suggested that CNP might inhibit particle assembly by binding directly to Gag. Importantly, the identification of an inactive point mutant CNP (D72E) and a CNP-resistant Gag point mutant (E40K) provided specificity controls to investigate this question. Our initial attempts to specifically coprecipitate CNP with a Gag-glutathione-S-transferase (GST) fusion protein, coexpressed in 293T cells, proved unsuccessful. However, when cells were treated with a crosslinking reagent (ethylene glycol bis[sulfosuccinimidylsuccinate], EGS) prior to glutathione-Sepharose precipitation, crosslinked CNP:Gag-GST complexes were readily detected in the precipitates (Figure 7D). The crosslinked proteins included one species of a size (~130 kDa) that suggested the formation of a complex containing only one CNP molecule (~48 kDa) and one Gag-GST (82 kDa) molecule, as well as higher molecular weight forms that may have contained multiple copies of Gag-GST and/or CNP or other proteins (Figure 7D). The apparent formation of a ~130 kDa 1:1 CNP:Gag-GST complex, using an EGS crosslinker that is only ~16 Å in length, strongly suggested that CNP and Gag-GST bound directly to each other. Importantly, the formation of the CNP:Gag-GST complexes was remarkably specific. Only trace amounts of CNP(D72E):Gag-GST or CNP:Gag(E40K)-GST complexes were formed (Figure 7D). Thus, the specificity with which CNP:Gag-GST complexes formed precisely recapitulated the specificity that the antiviral effects of CNP were observed.

The findings that CNP bound to Gag (Figure 7D), and impeded the coalescence of Gag-GFP fluorescent puncta (Figures 5F and 5G) led us to consider whether CNP might induce the accumulation of incomplete budding structures or misformed assembly intermediates that were not detectable by fluorescence microscopy. To examine this possibility, we utilized MT4 cells stably expressing CNP (Figures 6A–6C and Figures 7E). In this context, the CNP expression level is comparable to intermediate levels used in cotransfection experiments (Figure 7E) and causes submaximal inhibition of particle assembly. We reasoned that this condition would increase the likelihood of observing abnormal virions or assembly intermediates. CNP-expressing cells were infected with equivalent titers of CNP-sensitive (WT) or CNP-resistant (E40K) HIV-1 (both encoding GFP in place of *nef*) yielding ~65% infected cells (Figure S3A) and examined using thin section electron microscopy (Figures 7F–7H). The fraction of cells on which virions were observed was reduced ~2-fold in WT HIV-1 infected cells as compared to CNP-resistant (E40K) HIV-1 infected cells (Figure 7G). Moreover, when the number of virions associated with producing cells was counted, this number was ~5-fold reduced for WT HIV-1 infected cells as compared to CNP-resistant (E40K) HIV-1 infected cells (Figure 7H). Thus, the overall observed reduction in the number of virions observed in WT HIV-1 infected cells as compared to CNP-resistant (E40K) HIV-1 infected cells was ~10-fold, entirely consistent with the reduction in WT HIV-1 particle production observed in the same cells using western blot assays (Figure 7I). Importantly, the morphology of virions and budding structures were indistinguishable regardless of whether CNP-sensitive or -resistant viruses were considered. In particular, although WT virions were fewer in number than CNP-resistant virions, they were generally of the correct size and morphology (Figure S3B). These data suggest that when CNP successfully inhibits HIV-1 assembly it does so at an early stage, i.e., before electron dense structures (Figures 7F–7H) or fluorescent puncta (Figures 5F and 5G) become detectable. "Breakthrough" particles that do assemble in the presence of CNP apparently achieve normal morphology and infectiousness.

DISCUSSION

Here we report a function for the phosphodiesterase enzyme CNP, namely the ability to bind to Gag and potently block the assembly of HIV-1 and several other primate lentiviruses. CNP apparently inhibits assembly by binding to Gag in a highly specific manner, as single amino acid substitutions in either MA or CNP abolished both binding and antiviral activity. Notably, single amino acid substitutions in MA have previously been proposed to govern host-specific adaptation of HIV-1/SIVcpz to human versus chimpanzee hosts (Wain et al., 2007), but at a different position to E40K. Moreover, because human and chimpanzee CNP protein sequences are identical, CNP is unlikely to underlie that particular host adaptation.

Even though CNP apparently targets MA, it inhibited virion assembly at a step subsequent to Gag association with the plasma membrane. At this stage of the virus lifecycle, Gag molecules and the viral genome are poised to coalesce into nascent particles. Our findings suggest that high levels of CNP impede the normal higher-order multimerization of Gag molecules that accompanies particle formation. We speculate that inhibition is the result of a steric effect, whereby CNP-Gag interactions inhibit Gag multimerization. Because the CNP-resistant E40K MA mutant has lost the ability to bind CNP, and no longer colocalizes with CNP at the plasma membrane, it is likely that Gag-CNP binding recruits CNP to budding sites, and that the E40K mutation results in the loss of a CNP binding site on Gag. However, we cannot formally exclude the alternative possibility that E40K Gag preferentially assembles at membrane microdomains that have a paucity of CNP, and that this underlies the absence of interaction between CNP and E40K Gag.

Although CNP-like proteins are present in diverse eukaryotes (from yeast to man), they have clearly evolved to take on different biological functions. In yeast, a CNP ortholog is required in tRNA splicing, and CNP is expressed as part of a multifunctional enzyme that includes tRNA ligase, 5′-OH kinase, and CNP-like domains. In mammals, as in yeast, CNP is an enzyme that can catalyze the hydrolysis of 2′,3′-cyclic nucleotides to produce 2′-nucleotides (Sakamoto et al., 2005). However, CNP is not required for tRNA splicing in mammals, and lacks the RNA ligase domain. Indeed, the physiologically relevant substrate and the biological role of CNP in mammalian cells are unknown. The catalytic activity of CNP is dispensable for antiviral activity, but the absolute conservation of the H-X-T-X catalytic residues suggests that CNP has functions in addition to antiretroviral activity. In fact, mice lacking CNP expression suffer from neurodegeneration in later life and premature death (Lappe-Siefke et al., 2003), but the underlying causes of this phenotype are not known.

Although inhibitory expression levels of CNP in transfected cells are well within the levels observed in certain murine tissues in vivo (Figure 2), no cultured human cell lines express these high levels of CNP. Therefore, we were not able to address the role of
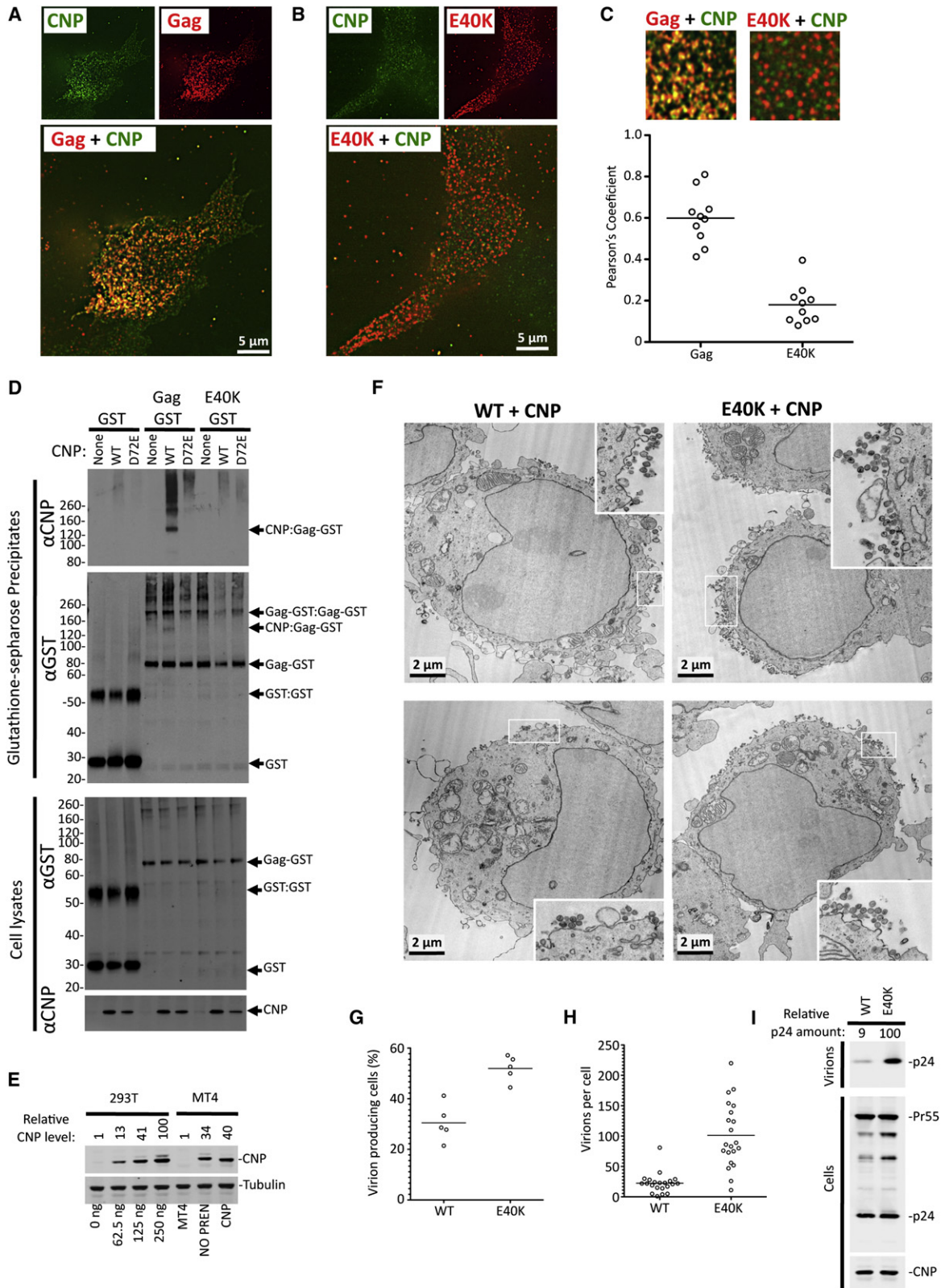
Figure 7. CNP Binds Gag and Inhibits HIV-1 Particle Production
(A and B) Representative images (acquired at the cell-coverslip interface) of 293T cells coexpressing CNP along with WT (A) or E40K (B) Gag and Gag-mCherry, and stained using Alex Fluor 488 labeled anti-CNP.

endogenously expressed CNP in limiting HIV-1 replication. Based on microarray analyses of human tissues, the only cells outside the brain that express significant levels of CNP are dendritic cells (Su et al., 2004). Thus it seems unlikely that CNP exerts strong inhibition of HIV-1 replication in vivo. It seems more likely that CNP is an "orphan" restriction factor whose antiviral potential is underexploited by the hosts of lentiviruses. If this is the case, then CNP exemplifies the huge antiviral potential of the mammalian genome, and it is possible that CNP constitutes part of the "raw material" from which restriction factors evolve. On the other hand, very little is known about the tropism of ancestral primate lentiviruses, and the discovery of an ancient endogenous SIV (that, by definition, infected germ-line cells) (Gifford et al., 2008) implies that acquisition of strict tropism of primate lentiviruses for CD4+ cells is a relatively recent occurrence. Thus, we speculate that CNP may have targeted ancient neurotropic lentiviruses, perhaps to protect the brain from damaging infection. Consistent with this idea, the simpler lentivirus, Maedi Visna virus, is oligodendrocyte-tropic (Stowring et al., 1985). In addition, beyond HIV-1, HIV-2, and SIV$_{MAC}$, little is known about neurotropism of primate lentiviruses in their normal hosts. It remains possible that some contemporary primate lentiviruses might exploit the oligodendrocyte niche and replicate in cells that express high levels of CNP.

The great interest in identifying and characterizing retroviral restriction factors in recent years has identified the recurrent theme that restriction factors must either be antagonized or avoided in their natural host. Evasion of a restriction factor could occur at the molecular level, for example by varying a protein surface to avoid restriction factors. Alternatively, viral tropism could be selected so as to avoid the restriction factor altogether. In the case of CNP, both evasion or avoidance strategies appear possible. At the molecular level, the occasional appearance of K40 (e.g., in SIV$_{AGM}$TAN) may be a means of evading CNP. Likewise, the tropism of primate lentiviruses might have evolved to avoid replication in cells expressing high levels of CNP.

In conclusion, CNP is a host protein that is clearly capable of inhibiting the assembly of HIV-1 and other primate lentiviruses. Although the identity of viruses that have been, are, or will be targeted by CNP remain elusive, this study illustrates an entirely unanticipated mechanism by which host factors can interfere with virus replication. Whether the antiviral potential provided by host gene products can be exploited or mimicked in the context of gene-based or pharmaceutical therapy remains to be determined.

EXPERIMENTAL PROCEDURES

Additional details of the experimental procedures are given in the Supplemental Experimental Procedures.

Plasmid Construction
The library of ISGs (Figure 1) were inserted into a CMV promoter-driven expression vector (pcDNA DEST40, Invitrogen) using the Gateway procedure, according to manufacturers instructions. CNP cDNAs from the various mammalian species were amplified by PCR and cloned using oligonucleotide derived SfiI sites into Gateway-compatible entry vectors prior to transfer to a CMV promoter-driven expression vector (pcDNA-DEST40, Invitrogen) for transfection. Mutant CNP expression plasmids, and a mutant HIV-1 proviral plasmid (NHG, that carries GFP in place of nef) bearing the E40K MA mutation, were generated using PCR-based mutagenesis and oligonucleotides detailed in the Supplemental Experimental Procedures.

Cell Lines and Transfection
Cell lines and peripheral blood mononuclear cells were maintained under standard conditions. MT-4 cell clones expressing CNP were generated by transduction with retroviral vectors, puromycin selection, and single cell cloning by limiting dilution. Clones were subsequently maintained in medium supplemented with puromycin. All transfection experiments were performed in 293T cells, which were seeded in 24-well plates at a concentration of 2.5×10^5 cells/well and transfected the following day using polyethylenimine (PolySciences).

Virus Release and Infectivity Assays
For the ISG screen (Figure 1), 293T cells were cotransfected with individual ISG expression vectors and plasmids required to make VSV-G-pseudotyped, GFP-expressing HIV-1 vector particles. In addition, a plasmid-expressing HA-GFP was also cotransfected.

To measure the effect of CNP on virus particle production, cells were transfected with increasing or fixed amounts of a CNP expression plasmid along with plasmids required to generate infectious retrovirus particles or VLPs.

In all transfection experiments, the total amount of DNA was held constant within the experiment by supplementing the transfection with an empty expression vector. At 48 hr posttransfection, virion-containing culture supernatants were harvested, clarified by low speed centrifugation, and filtered (0.22 μm). Particle release was evaluated using western blot analysis of cell lysates and pelleted virions using an anti HIV-1 p24 CA antibody. Infectious virions were quantified by inoculating TZM-bl indicator cells followed by β-galactosidase assay or, in cases where the viral genome encoded GFP, by inoculating MT4 cells and enumerating infected cells by FACS.

HIV-1 Adaptation and Replication Assays
MT4 cells were infected with HIV-1 (NHG) and infection monitored by FACS analysis. Culture supernatants were used to inoculate fresh MT4 cells when the majority of the cells became infected. Replication of WT or E40K mutant HIV-1 in human peripheral blood mononuclear cells was monitored using reverse transcriptase assays.

(C) Quantitative analysis of colocalization. Each symbol in the graph is the Pearson's coefficient for an individual cell and the horizontal line represents the mean value. Expanded images from the cell-coverslip interface are also shown.

(D) Western blot analysis (αCNP or αGST) of glutathione-Sepharose precipitates and cell lysates from crosslinker-treated 293T cells, coexpressing the indicated WT or mutant CNP, GST, or Gag-GST proteins. Molecular weight markers indicate the mass in kDa.

(E) Quantitative western blot analysis of 293T cells transiently transfected with the indicated amount of a CNP expression vector (from Figure 2B) and MT4 cells stably expressing CNP. Numbers above each lane indicate the relative band intensities (LiCOR).

(F) Electron microscopic images of CNP expressing MT4 cells infected with HIV-1, or the CNP-resistant HIV-1 point mutant E40K, 48 hr postinfection (two representative images for each are shown).

(G) Percentage of infected cells that exhibited associated virions. One square of a 200 mesh grid (∼20 cells) was counted for each data point.

(H) Quantification of the number of virions and budding structures on infected MT4 cells. Each data point represents an individual cell, and only cells that exhibited associated virions were evaluated.

(I) Quantitative western blot analysis of virion yield, CNP, and Gag expression in MT4 CNP cells identically infected in parallel with those used in (F–H). Numbers above each lane indicate the relative band intensities (LiCOR). See also Figure S3.

Western Blot Analyses

Glutathione-Sepharose precipitates, virion and cell lysates, or tissue extracts were separated on 4%–12% acrylamide gels, blotted onto nitrocellulose membranes, and probed with anti-HIV-1-p24CA (183-H12-5C), anti-CNP (Millipore), or anti-tubulin primary antibodies (Sigma).

Subsequently, blots were probed with peroxidase-labeled goat anti-mouse antibodies or with fluorescent goat anti-mouse IRdye 800CW antibodies (Li-COR) prior to visualization by exposure to film or quantitation using an Odyssey infrared imaging system (Li-COR).

CNP Expression in Tissues

Tissues from 16-day-old and 1-day-old C57BL/6 mice were harvested, and digested where necessary with proteinase K prior to isolating single-cell suspensions using a cell strainer. The tissue samples were then lysed in RIPA buffer (150 mM NaCl, 50 mM Tris [pH 7.4], 0.1% SDS, 1 mM EDTA, 1% Igepal CA-630, 1% Na deoxycholate, and protease inhibitors), diluted in protein sample buffer, and sonicated. CNP expression was assessed by western blotting as described above.

Membrane Flotation Assay

Cells expressing HIV-1 Gag, a packageable viral genome and CNP were generated by transfection of HEK293T cells with a vector genome expressing plasmid (V1B) (Kutluay and Bieniasz, 2010) along with plasmids expressing Gag and CNP. They were then subjected to membrane flotation assay as previously described (Kutluay and Bieniasz, 2010; Spearman et al., 1997) (as detailed in the Supplemental Experimental Procedures). Gradient fractions were probed for the presence of Gag and CNP proteins using western blot assays, as well as viral RNA, using quantitative RT PCR assays as described previously (Kutluay and Bieniasz, 2010).

Fluorescent and Electron Microscopy

Cells, seeded in glass-bottomed dishes were transfected with HIV-1 Gag, Gag-GFP, Gag-mCherry, and CNP expression vectors. They were then immunostained where necessary, using an anti-CNP antibody and observed by deconvolution microscopy, as described previously (Jouvenet et al., 2006). Puncta of Gag-GFP from randomly selected fields were counted and Pearson's colocalization coefficients derived, as described in the Supplemental Experimental Procedures. Thin section EM of HIV-1-infected MT4 cells was carried out using previously described methods (Zhang et al., 2009), as detailed in the Supplemental Experimental Procedures. The number of virions per cell was determined by counting the number of virus like structures (virions and budding structures) per cell, using randomly selected cells that were adjudged to have at least one definitive virus-like structure. The percentage of virion producing cells per square of a 200 Mesh EM grid was calculated by counting the number of cells with or without definitive associated virion structures. Approximately 20 cells each from five different squares (a total of ~100 cells) were sampled for each condition.

Crosslinking and Precipitation Analyses

293T cells expressing CNP and Gag-GST were treated with ethylene glycol bis[succinimidylsuccinate] (EGS) crosslinker, and glutathione-Sepharose precipitates prepared as previously described (Eastman et al., 2005; Kutluay and Bieniasz, 2010). The precipitates were analyzed by western blotting, as described above.

Analysis of Protein Incorporation into Virions

To assess the incorporation of Env protein or CNP into virions, virions were harvested from transfected 293T cells and subjected to western blot analysis, as described above, and detailed in the Supplemental Experimental Procedures. To assess whether CNP was incorporated into the interior of particles, purified virions were treated with subtilisin prior to western blot analysis, as detailed in the Supplemental Experimental Procedures.

For mass spectrometry analysis of virions, particles were harvested from the supernatant of infected 293T cells by ultracentrifugation onto a sucrose cushion, then separated on an Optiprep gradient. Proteins in each of ten gradient fractions were precipitated with trichloroacetic acid and separated by gel electrophoresis. A fraction containing the majority of the virions was identified, and gel pieces comprising the entire lane were analyzed using

a using an Orbitrap XL mass spectrometer, as described in the Supplemental Experimental Procedures.

REFERENCES

Bartee, E., Mohamed, M.R., Lopez, M.C., Baker, H.V., and McFadden, G. (2009). The addition of tumor necrosis factor plus beta interferon induces a novel synergistic antiviral state against poxviruses in primary human fibroblasts. J. Virol. *83*, 498–511.

Bryant, M., and Ratner, L. (1990). Myristoylation-dependent replication and assembly of human immunodeficiency virus 1. Proc. Natl. Acad. Sci. USA *87*, 523–527.

Chertova, E., Chertov, O., Coren, L.V., Roser, J.D., Trubey, C.M., Bess, J.W., Jr., Sowder, R.C., 2nd, Barsov, E., Hood, B.L., Fisher, R.J., et al. (2006). Proteomic and biochemical analysis of purified human immunodeficiency virus type 1 produced from infected monocyte-derived macrophages. J. Virol. *80*, 9039–9052.

Eastman, S.W., Martin-Serrano, J., Chung, W., Zang, T., and Bieniasz, P.D. (2005). Identification of human VPS37C, a component of endosomal sorting complex required for transport-I important for viral budding. J. Biol. Chem. *280*, 628–636.

Furtak, V., Mulky, A., Rawlings, S.A., Kozhaya, L., Lee, K., Kewalramani, V.N., and Unutmaz, D. (2010). Perturbation of the P-body component Mov10 inhibits HIV-1 infectivity. PLoS ONE *5*, e9081.

Gao, G., Guo, X., and Goff, S.P. (2002). Inhibition of retroviral RNA production by ZAP, a CCCH-type zinc finger protein. Science *297*, 1703–1706.

Gifford, R.J., Katzourakis, A., Tristem, M., Pybus, O.G., Winters, M., and Shafer, R.W. (2008). A transitional endogenous lentivirus from the genome of a basal primate and implications for lentivirus evolution. Proc. Natl. Acad. Sci. USA *105*, 20362–20367.

Hill, C.P., Worthylake, D., Bancroft, D.P., Christensen, A.M., and Sundquist, W.I. (1996). Crystal structures of the trimeric human immunodeficiency virus type 1 matrix protein: implications for membrane association and assembly. Proc. Natl. Acad. Sci. USA *93*, 3099–3104.

Ho, D.D., Hartshorn, K.L., Rota, T.R., Andrews, C.A., Kaplan, J.C., Schooley, R.T., and Hirsch, M.S. (1985). Recombinant human interferon alfa-A suppresses HTLV-III replication in vitro. Lancet *1*, 602–604.

Jouvenet, N., Neil, S.J., Bess, C., Johnson, M.C., Virgen, C.A., Simon, S.M., and Bieniasz, P.D. (2006). Plasma membrane is the site of productive HIV-1 particle assembly. PLoS Biol. *4*, e435.

Jouvenet, N., Bieniasz, P.D., and Simon, S.M. (2008). Imaging the biogenesis of individual HIV-1 virions in live cells. Nature *454*, 236–240.

Kirmaier, A., Wu, F., Newman, R.M., Hall, L.R., Morgan, J.S., O'Connor, S., Marx, P.A., Meythaler, M., Goldstein, S., Buckler-White, A., et al. (2010). TRIM5 suppresses cross-species transmission of a primate immunodeficiency virus and selects for emergence of resistant variants in the new species. PLoS Biol. *8*, 8.

Kutluay, S.B., and Bieniasz, P.D. (2010). Analysis of the initiating events in HIV-1 particle assembly and genome packaging. PLoS Pathog. *6*, e1001200.

Lappe-Siefke, C., Goebbels, S., Gravel, M., Nicksch, E., Lee, J., Braun, P.E., Griffiths, I.R., and Nave, K.A. (2003). Disruption of Cnp1 uncouples oligodendroglial functions in axonal support and myelination. Nat. Genet. *33*, 366–374.

Larson, D.R., Johnson, M.C., Webb, W.W., and Vogt, V.M. (2005). Visualization of retrovirus budding with correlated light and electron microscopy. Proc. Natl. Acad. Sci. USA *102*, 15453–15458.

Lee, J., Gravel, M., Gao, E., O'Neill, R.C., and Braun, P.E. (2001). Identification of essential residues in 2′,3′-cyclic nucleotide 3′-phosphodiesterase. Chemical modification and site-directed mutagenesis to investigate the role of cysteine and histidine residues in enzymatic activity. J. Biol. Chem. *276*, 14804–14813.

Liberatore, R.A., and Bieniasz, P.D. (2011). Tetherin is a key effector of the antiretroviral activity of type I interferon in vitro and in vivo. Proc. Natl. Acad. Sci. USA *108*, 18097–18101.

McNatt, M.W., Zang, T., Hatziioannou, T., Bartlett, M., Fofana, I.B., Johnson, W.E., Neil, S.J., and Bieniasz, P.D. (2009). Species-specific activity of HIV-1 Vpu and positive selection of tetherin transmembrane domain variants. PLoS Pathog. *5*, e1000300.

Neil, S.J., Zang, T., and Bieniasz, P.D. (2008). Tetherin inhibits retrovirus release and is antagonized by HIV-1 Vpu. Nature *451*, 425–430.

O'Neill, R.C., Minuk, J., Cox, M.E., Braun, P.E., and Gravel, M. (1997). CNP2 mRNA directs synthesis of both CNP1 and CNP2 polypeptides. J. Neurosci. Res. *50*, 248–257.

Okeoma, C.M., Lovsin, N., Peterlin, B.M., and Ross, S.R. (2007). APOBEC3 inhibits mouse mammary tumour virus replication in vivo. Nature *445*, 927–930.

Pelvig, D.P., Pakkenberg, H., Stark, A.K., and Pakkenberg, B. (2008). Neocortical glial cell numbers in human brains. Neurobiol. Aging *29*, 1754–1762.

Perez-Caballero, D., Hatziioannou, T., Martin-Serrano, J., and Bieniasz, P.D. (2004). Human immunodeficiency virus type 1 matrix inhibits and confers cooperativity on gag precursor-membrane interactions. J. Virol. *78*, 9560–9563.

Sakamoto, Y., Tanaka, N., Ichimiya, T., Kurihara, T., and Nakamura, K.T. (2005). Crystal structure of the catalytic fragment of human brain 2′,3′-cyclic-nucleotide 3′-phosphodiesterase. J. Mol. Biol. *346*, 789–800.

Schoggins, J.W., Wilson, S.J., Panis, M., Murphy, M.Y., Jones, C.T., Bieniasz, P., and Rice, C.M. (2011). A diverse range of gene products are effectors of the type I interferon antiviral response. Nature *472*, 481–485.

Sheehy, A.M., Gaddis, N.C., Choi, J.D., and Malim, M.H. (2002). Isolation of a human gene that inhibits HIV-1 infection and is suppressed by the viral Vif protein. Nature *418*, 646–650.

Spearman, P., Horton, R., Ratner, L., and Kuli-Zade, I. (1997). Membrane binding of human immunodeficiency virus type 1 matrix protein in vivo supports a conformational myristyl switch mechanism. J. Virol. *71*, 6582–6592.

Stowring, L., Haase, A.T., Petursson, G., Georgsson, G., Palsson, P., Lutley, R., Roos, R., and Szuchet, S. (1985). Detection of visna virus antigens and RNA in glial cells in foci of demyelination. Virology *141*, 311–318.

Su, A.I., Wiltshire, T., Batalov, S., Lapp, H., Ching, K.A., Block, D., Zhang, J., Soden, R., Hayakawa, M., Kreiman, G., et al. (2004). A gene atlas of the mouse and human protein-encoding transcriptomes. Proc. Natl. Acad. Sci. USA *101*, 6062–6067.

Tang, C., Loeliger, E., Luncsford, P., Kinde, I., Beckett, D., and Summers, M.F. (2004). Entropic switch regulates myristate exposure in the HIV-1 matrix protein. Proc. Natl. Acad. Sci. USA *101*, 517–522.

Vogel, U.S., and Thompson, R.J. (1988). Molecular structure, localization, and possible functions of the myelin-associated enzyme 2′,3′-cyclic nucleotide 3′-phosphodiesterase. J. Neurochem. *50*, 1667–1677.

Wain, L.V., Bailes, E., Bibollet-Ruche, F., Decker, J.M., Keele, B.F., Van Heuverswyn, F., Li, Y., Takehisa, J., Ngole, E.M., Shaw, G.M., et al. (2007). Adaptation of HIV-1 to its human host. Mol. Biol. Evol. *24*, 1853–1860.

Zhang, F., Wilson, S.J., Landford, W.C., Virgen, B., Gregory, D., Johnson, M.C., Munch, J., Kirchhoff, F., Bieniasz, P.D., and Hatziioannou, T. (2009). Nef proteins from simian immunodeficiency viruses are tetherin antagonists. Cell Host Microbe *6*, 54–67.